Cognitive-enhancing effect of *Cordia dichotoma* fruit on scopolamine-induced cognitive impairment in rats: metabolite profiling, *in vivo*, and *in silico* investigations

Hagar M. Hussein[1], Mostafa A. Abdel Kawy[1], Basma M. Eltanany[2], Laura Pont[3,4], Fernando Benavente[3], Ahmed M. Fayez[5], Radwan Alnajjar[6,7], Ahmed A. Al-Karmalawy[8,9,] Azza R. Abdelmonem[1], Engy Mohsen[1]

[1]Department of Pharmacognosy, Faculty of Pharmacy, Cairo University, Cairo 11562, Egypt

[2] Department of Pharmaceutical Analytical Chemistry, Faculty of Pharmacy, Cairo University, Cairo 11562, Egypt

[3] Department of Chemical Engineering and Analytical Chemistry, Institute for Research on Nutrition and Food Safety (INSA·UB), University of Barcelona, Barcelona 08028, Spain

[4] Serra Húnter Program, Generalitat de Catalunya, Barcelona 08007, Spain

[5] School of Life and Medical Sciences, University of Hertfordshire Hosted by Global Academic Foundation, New Administrative Capital, Cairo11835, Egypt.

[6] Computer-aided drug design (CADD) Unit, Faculty of Pharmacy, Libyan International Medical University, Benghazi, Libya.

[7] Department of Chemistry, Faculty of Science, University of Benghazi, Benghazi, Libya.

[8]Department of Pharmaceutical Chemistry, College of Pharmacy, The University of Mashreq, Baghdad 10023, Iraq.

[9]Department of Pharmaceutical Chemistry, Faculty of Pharmacy, Horus University-Egypt, New Damietta 34518, Egypt.

*Corresponding author: Hagar M. Hussein (hagar.elhag@pharma.cu.edu.eg)

Supplementary Data. Materials and Methods

S1. Molecular dynamics simulations

Molecular dynamics simulations were carried out using Desmond simulation package of the Schrödinger LLCm. The NPT ensemble with the temperature 300 K and a pressure 1 bar was applied in all runs. The simulation length was 200 ns with a relaxation time of 1 ps for the ligands. The OPLS3 force field parameters were used in all simulations [1]. The cutoff radius in Coulomb interactions was 9.0 Å. The orthorhombic periodic box boundaries were set 10 Å away from the protein atoms. The water molecules were explicitly described using the transferable intermolecular potential with three points (TIP3P) model.[2,3]Salt concentration was set to 0.15 M NaCl and was built using the System Builder utility of the Desmond package. The Martyna−Tuckerman−Klein chain coupling scheme with a coupling constant of 2.0 ps was used for the pressure control and the Nosé−Hoover chain coupling scheme for the temperature control.[4,5] Nonbonded forces were calculated using a RESPA integrator, where the short-range forces were updated every step and the long-range forces were updated every three steps. The trajectories were saved at 20 ns intervals for analysis. The behavior and interactions between the protein and ligands were analyzed using the Simulation Interaction Diagram tool of the Desmond package. The stability of the simulations was monitored by monitoring the RMSD of the ligand and protein atom positions over time.

S2. Molecular dynamics trajectory analysis and prime molecular mechanics with generalized Born and surface area solvation calculations

Simulation interactions diagram panel of Maestro software was used to monitor contribution of the interactions in the ligand-protein stability. The molecular mechanics generalized Born/solvent accessibility (MM – GBSA) was performed to calculate the ligand binding free energies and ligand strain energies for docked compounds over the last 50 ns with thermal_mmgbsa.py python script provided by the Schrodinger platform. The script takes a Desmond trajectory file, splits it into individual snapshots, runs the MM-GBSA calculations on each frame, and outputs the average computed binding energy.

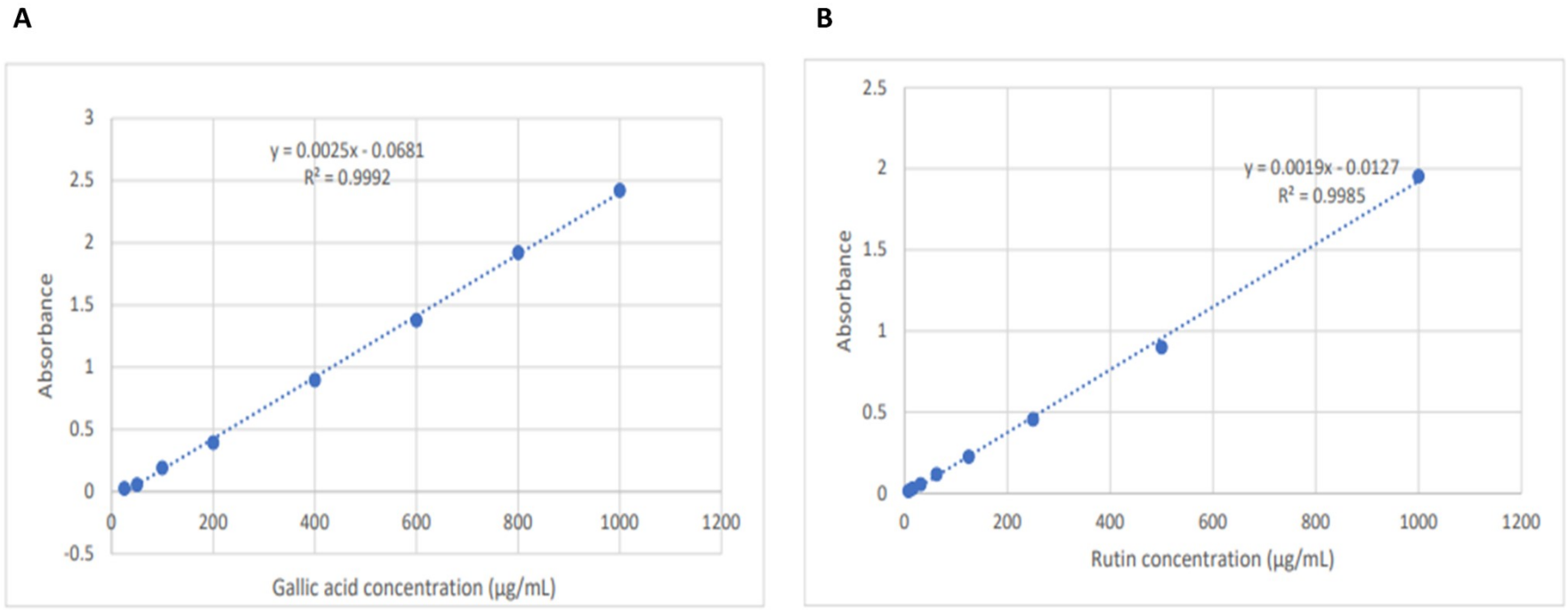

Fig. S1. Calibration curve of (**A**) gallic acid standard for the total phenolic content analysis, (**B**) and rutin standard for the total flavonoid content analysis

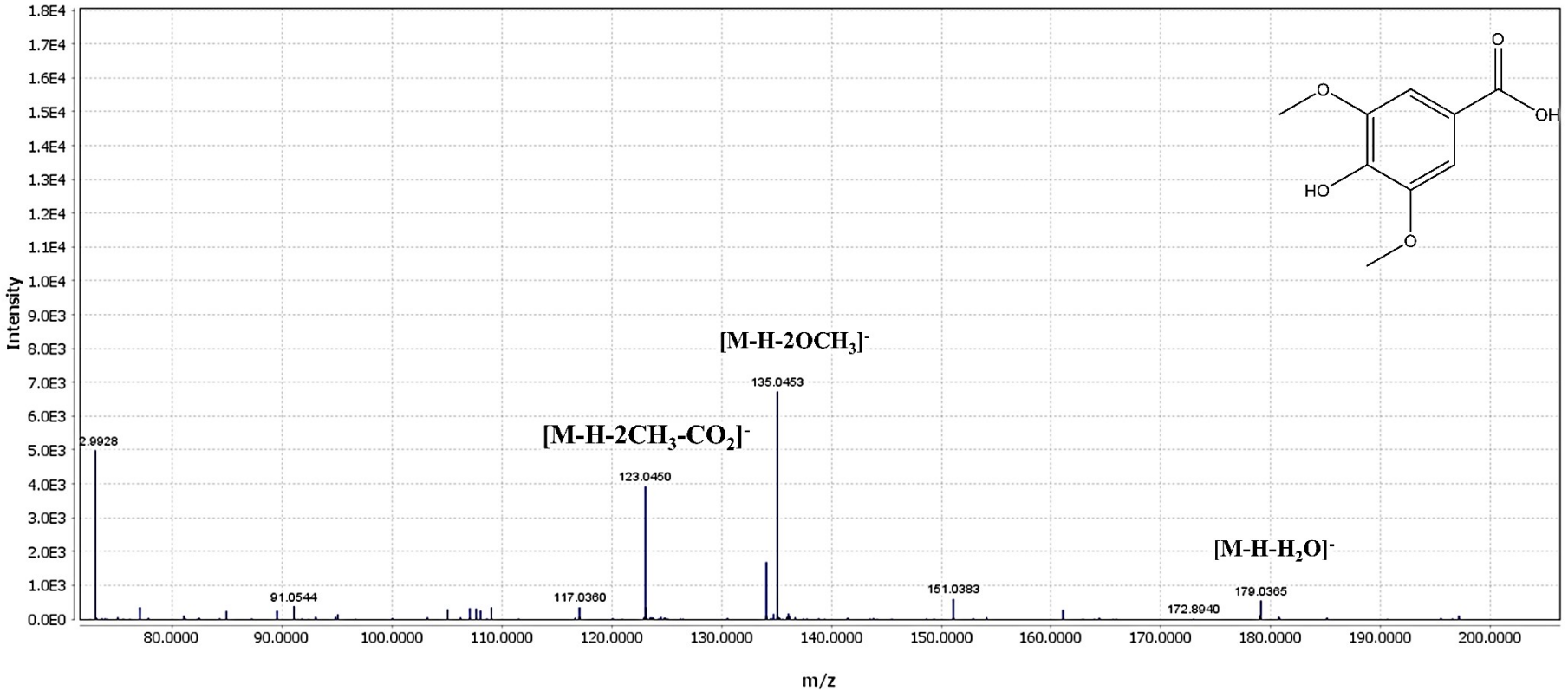

Fig. S2. MS/MS spectrum of syringic acid **(15, Table 1).**

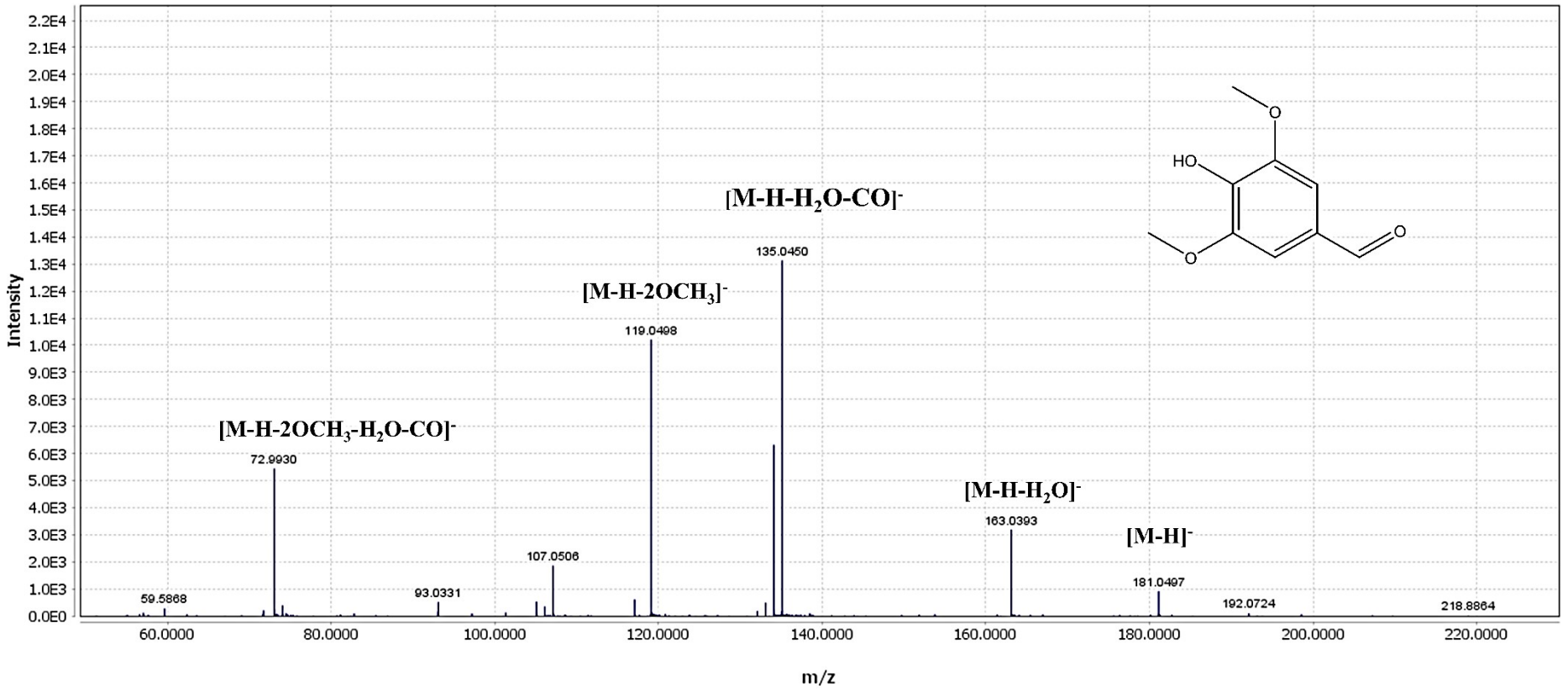

Fig. S3. MS/MS spectrum of syringaldehyde **(16, Table 1).**

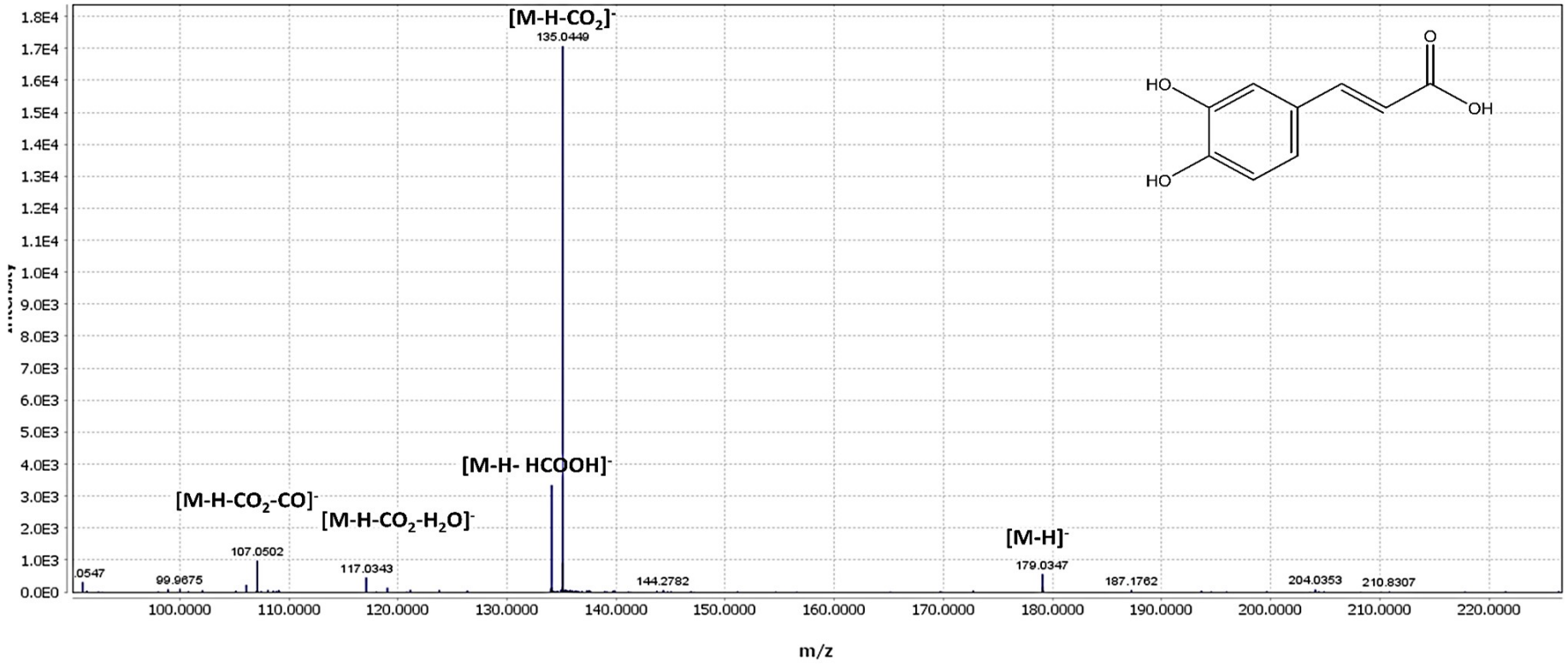

Fig. S4. MS/MS spectrum of caffeic acid **(19, Table 1).**

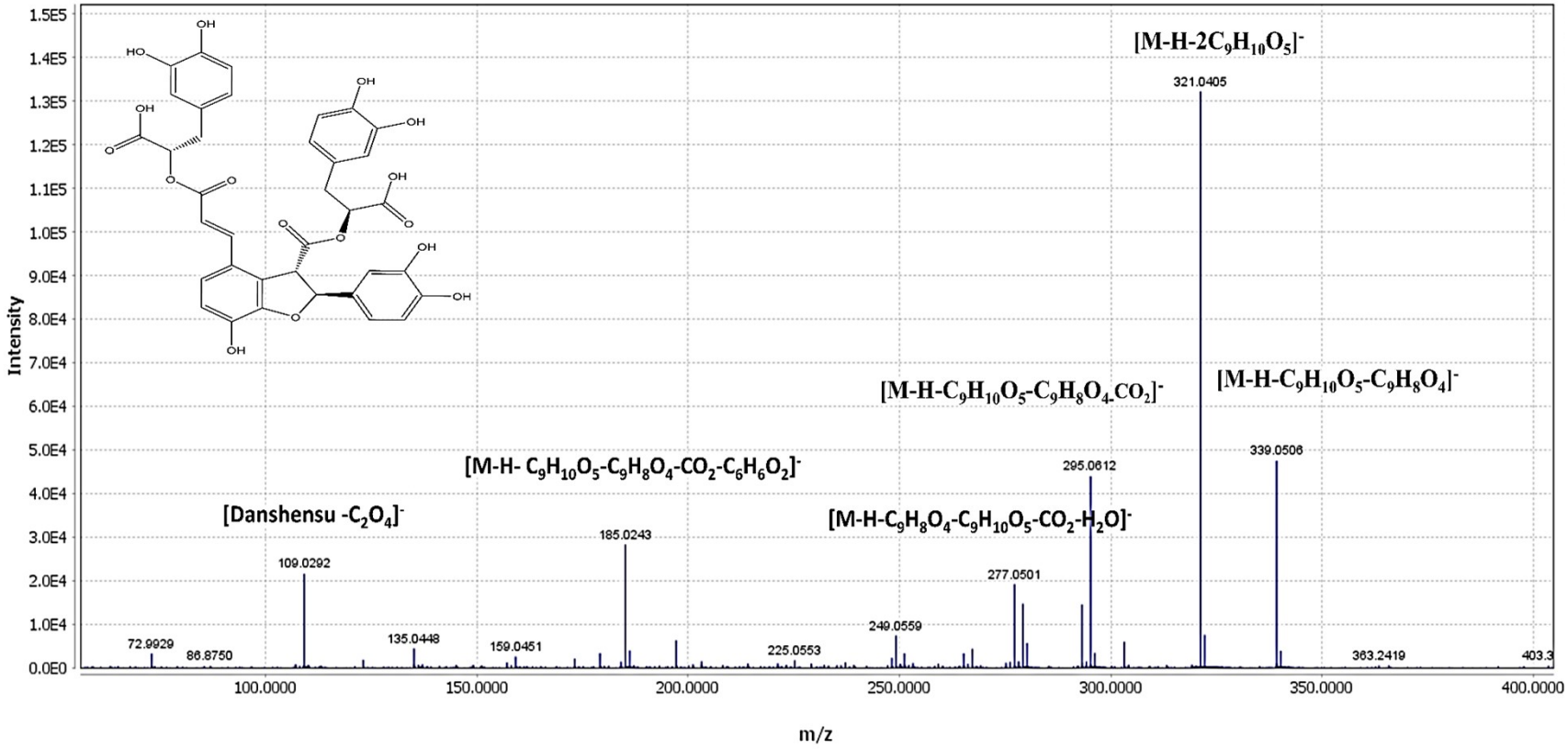

Fig. S5. MS/MS spectrum of salvianolic acid B **(24, Table 1).**

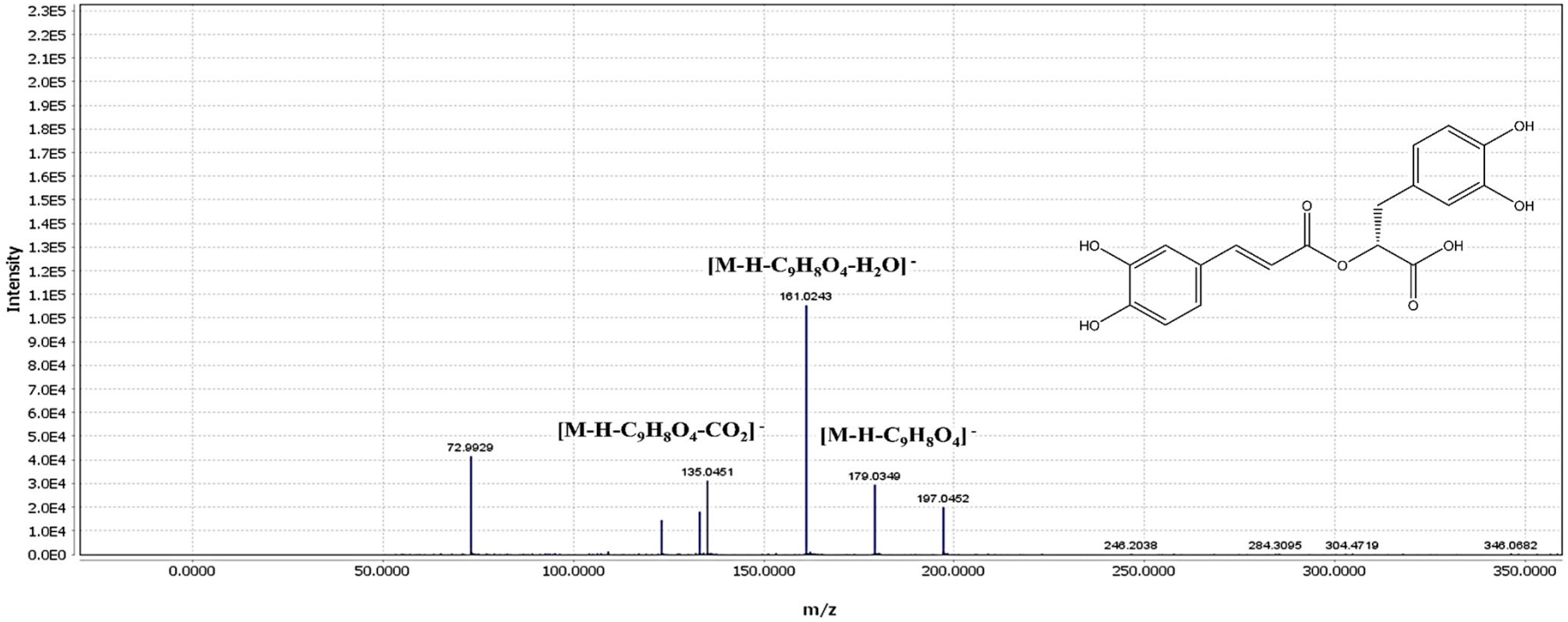

Fig. S6. MS/MS spectrum of rosmarinic acid **(27, Table 1).**

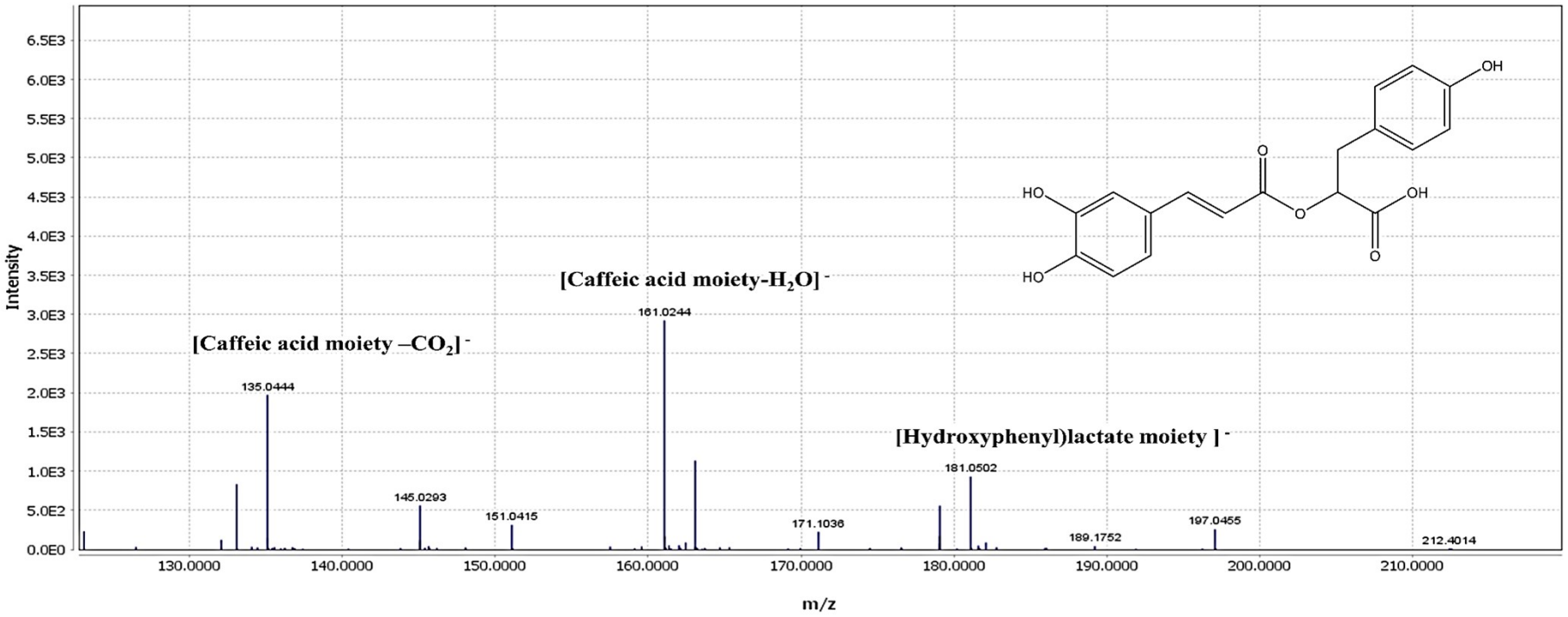

Fig. S7. MS/MS spectrum of Caffeoyl-4'-hydroxyphenyllactate (**34, table 1**)

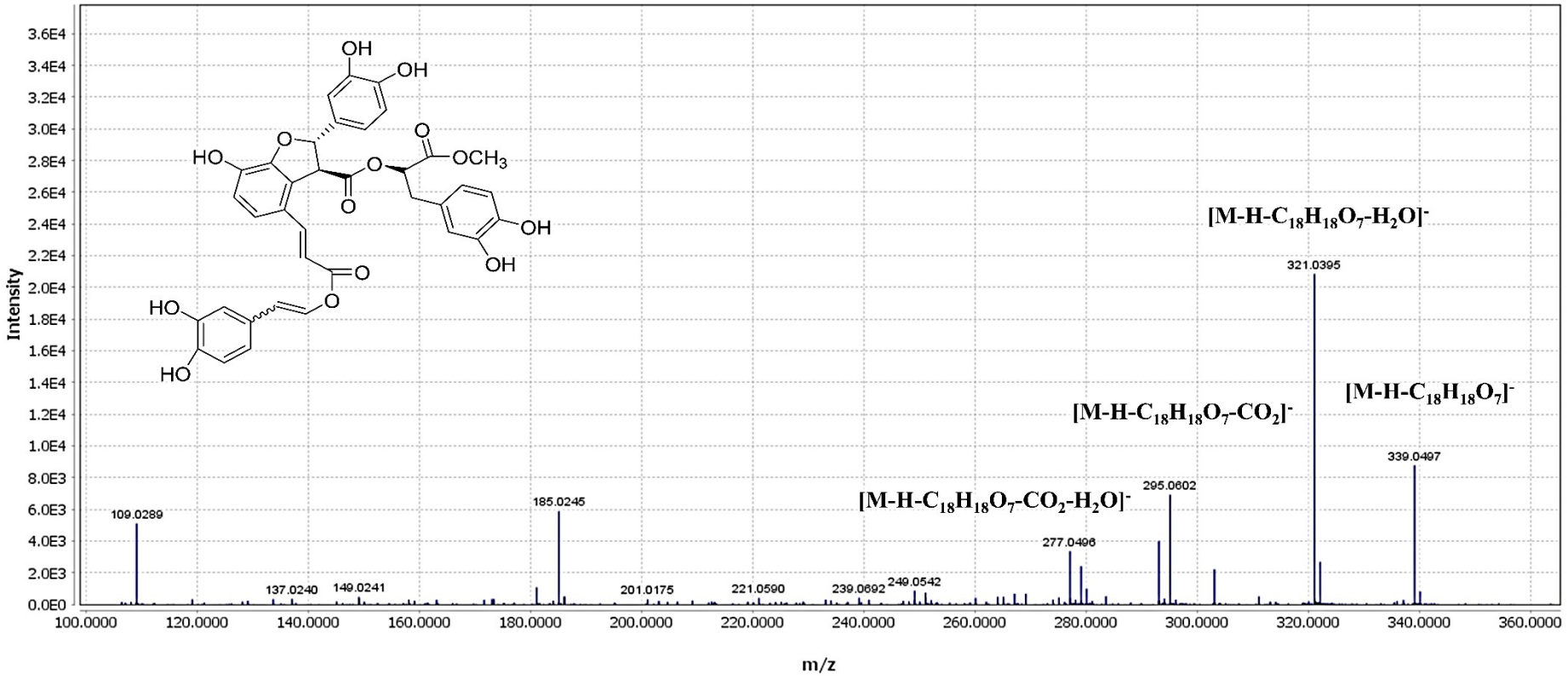

Fig. S8. MS/MS spectrum of sebestenoid C **(37, Table 1).**

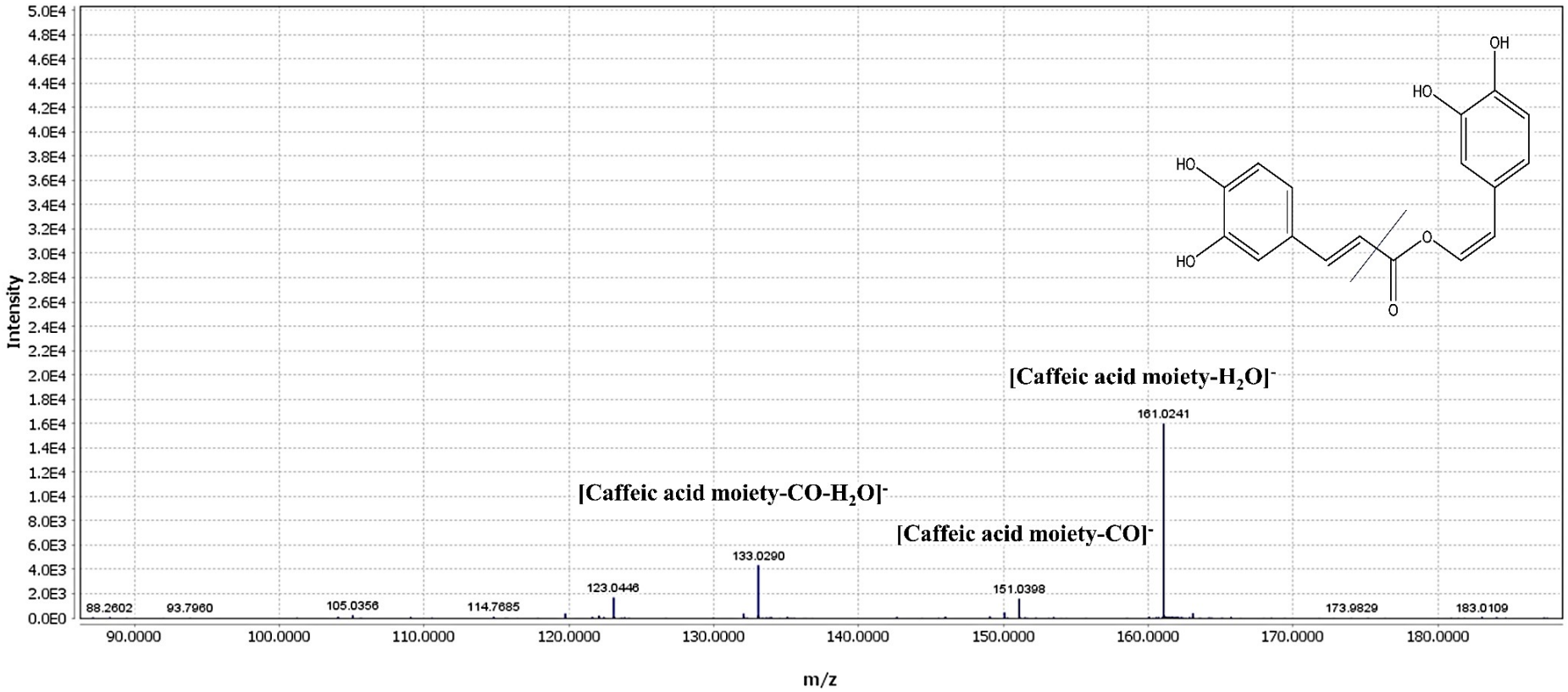

Fig. S9. MS/MS spectrum of nepetoidin B **(39 and 40, Table 1).**

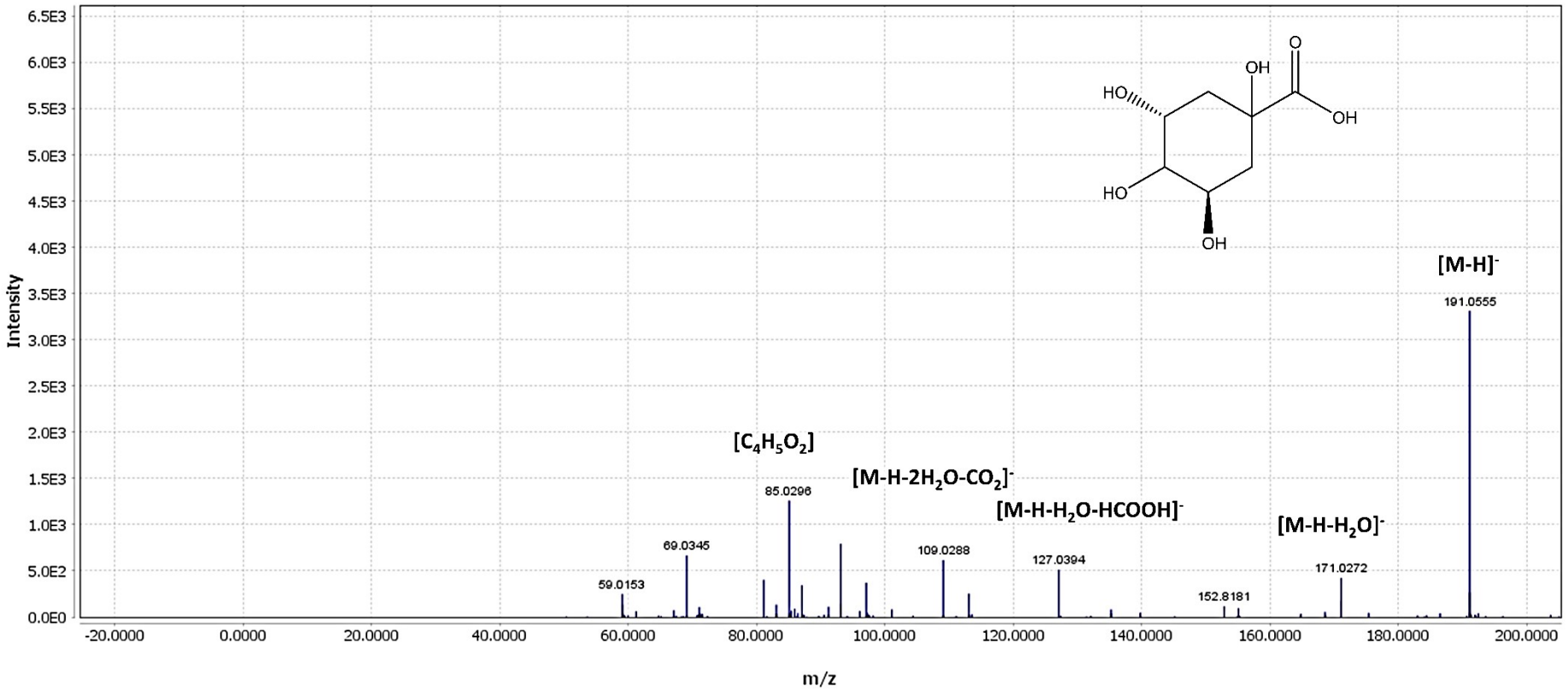

Fig. S10. MS/MS spectrum of quinic acid **(3, Table 1).**

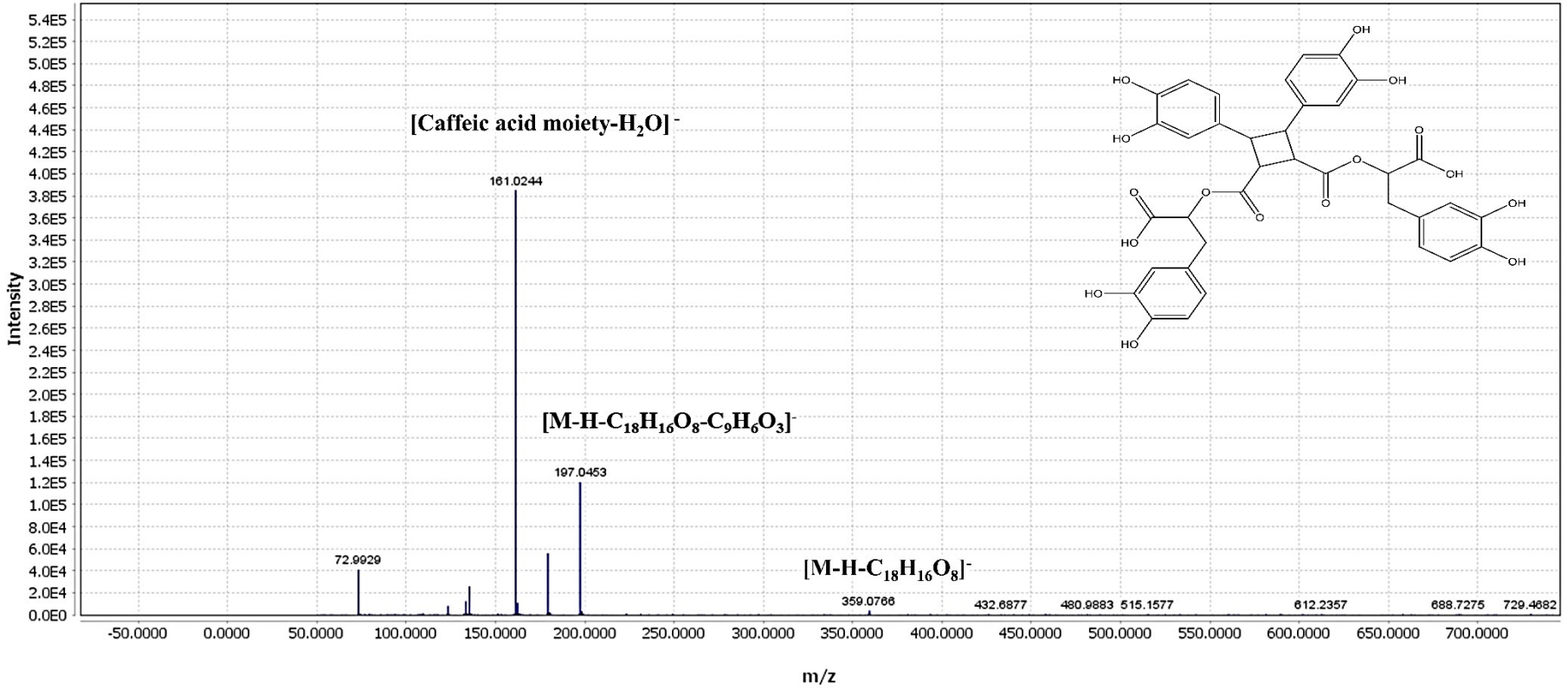

Fig. S11. MS/MS spectrum of sagerinic acid (**26, Table 1**).

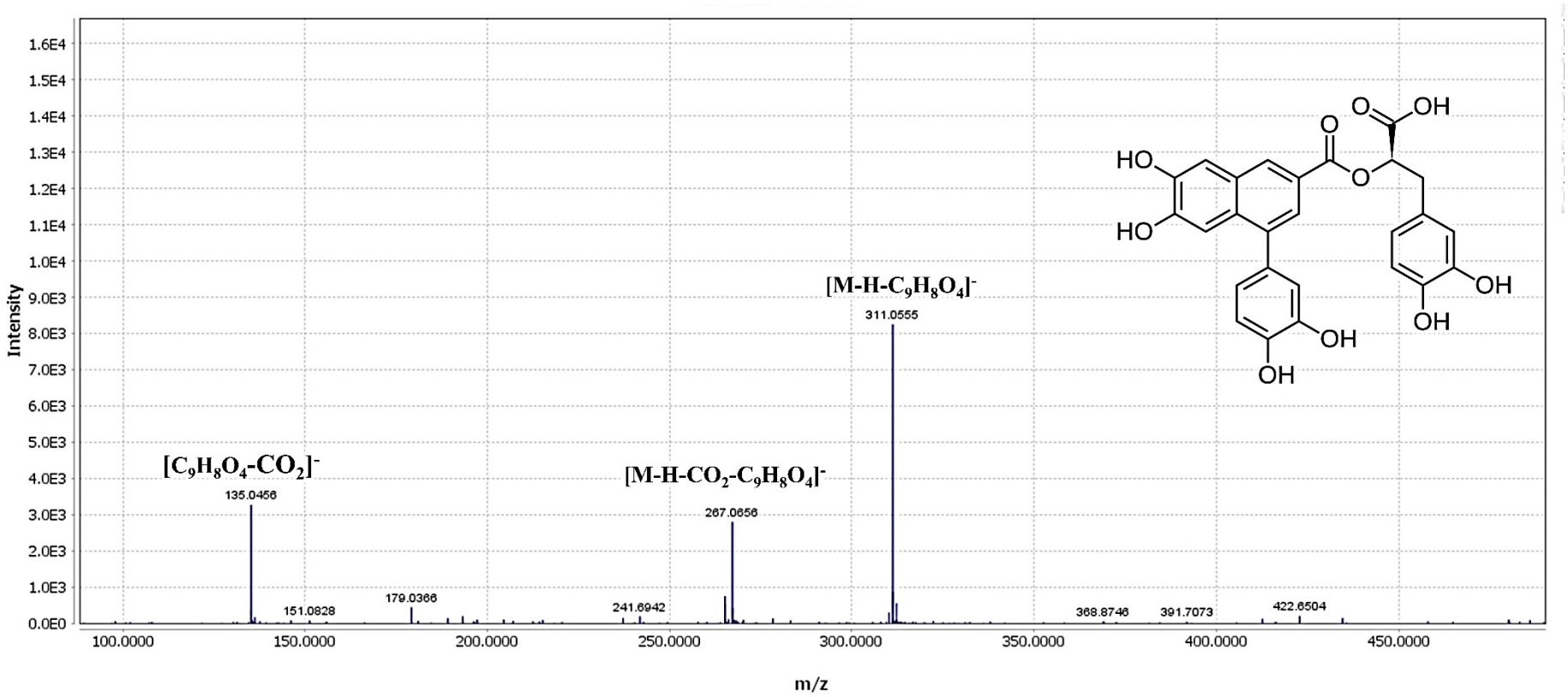

Fig. S12. MS/MS spectrum of globoidnan A (**32, Table 1**).

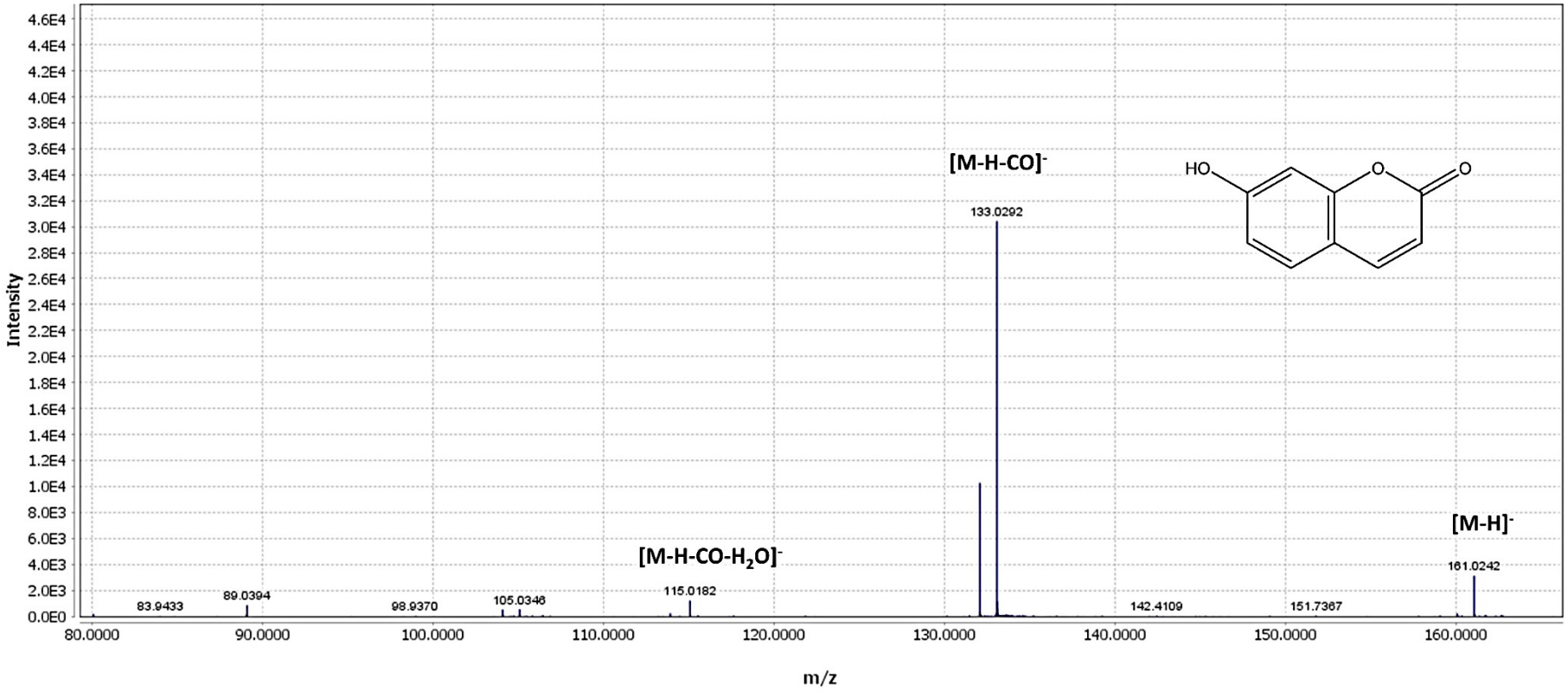

Fig. S13. MS/MS spectrum of hydroxycoumarin (**29, Table 1**).

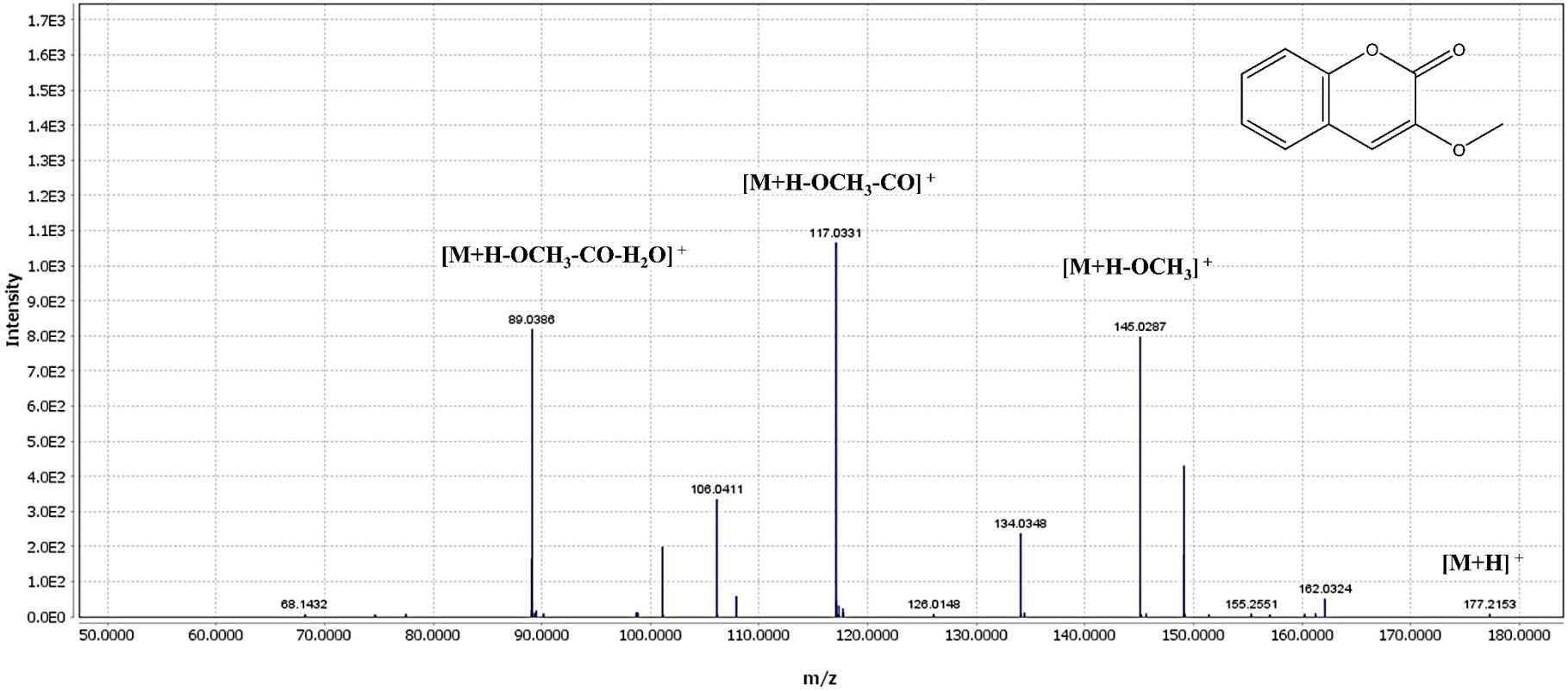

Fig. S14. MS/MS spectrum of methoxy coumarin (**36, Table 1**).

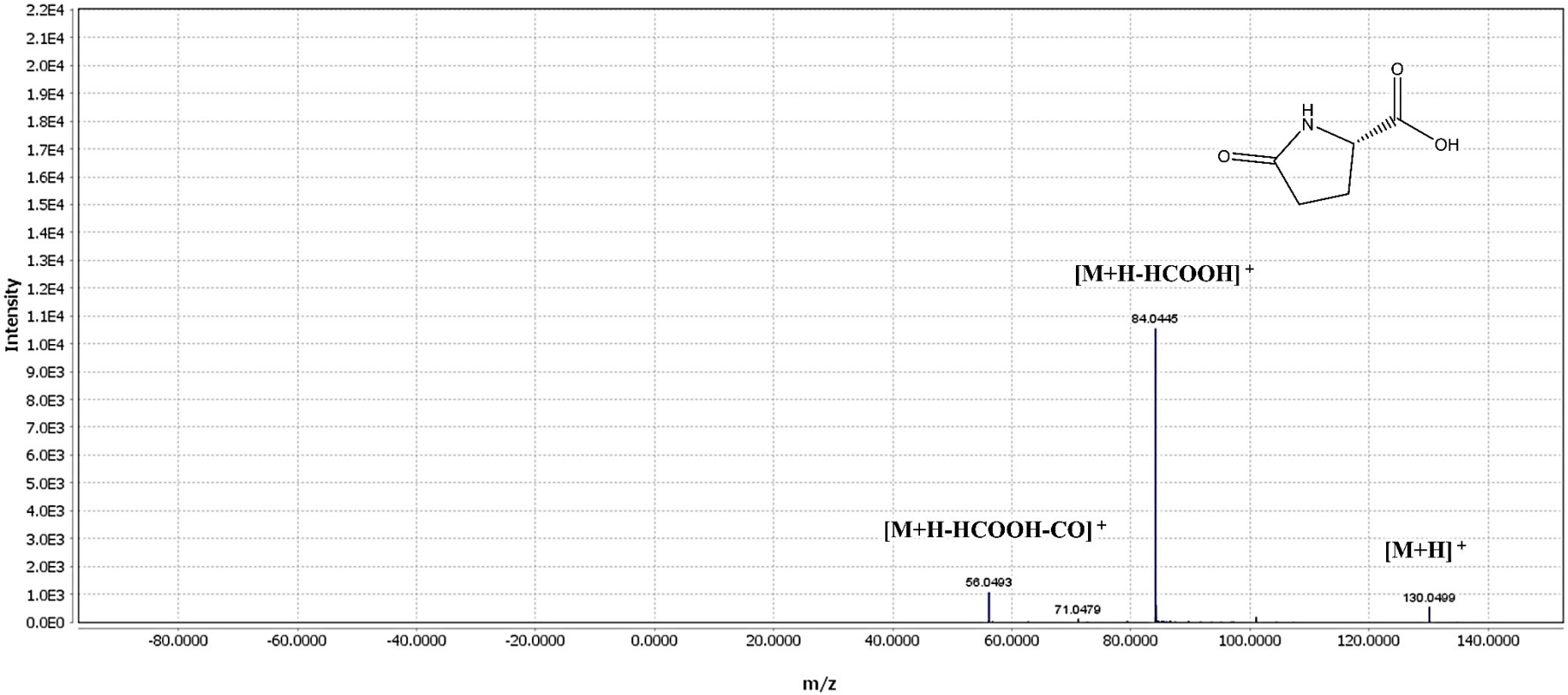

Fig. S15. MS/MS spectrum of pyroglutamic acid (**11, Table 1**).

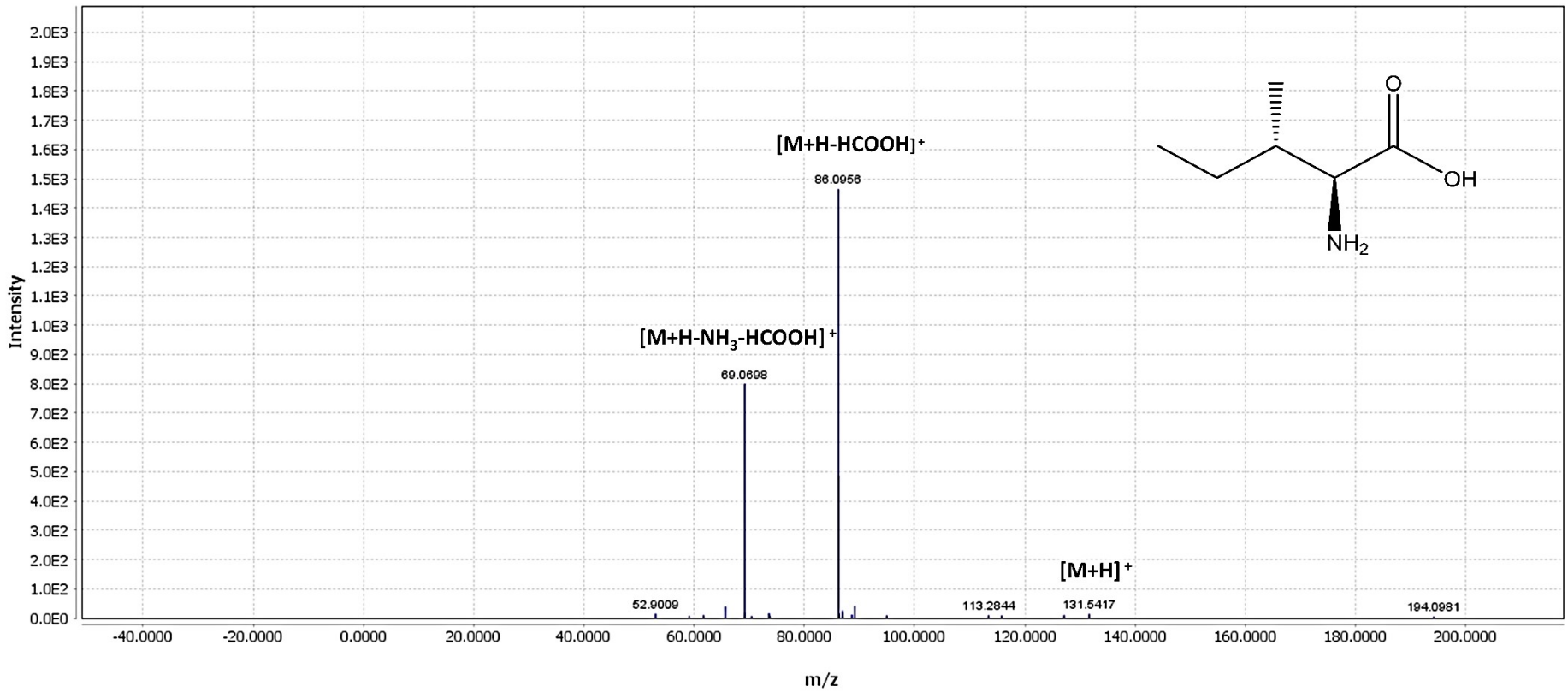

Fig. S16. MS/MS spectrum of isoleucine or leucine (**13, Table 1**).

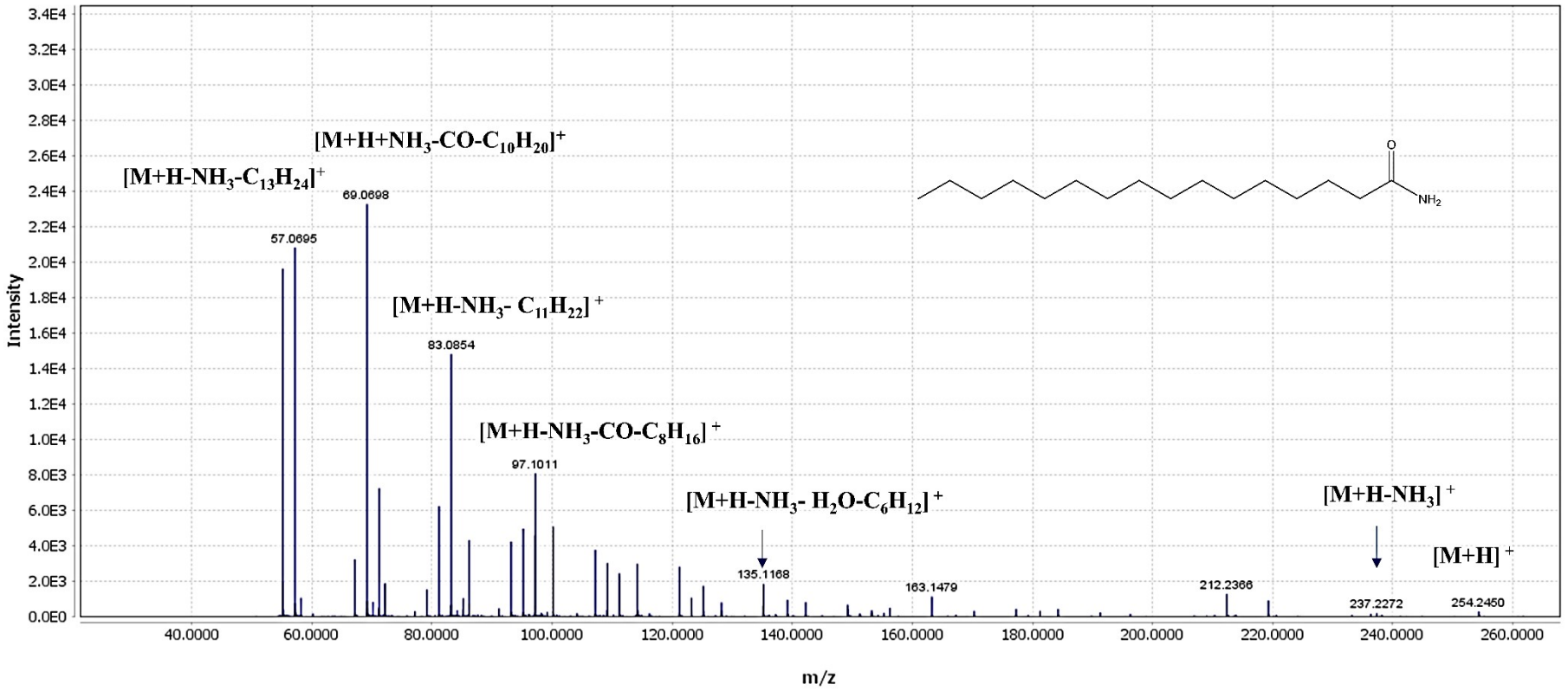

Fig. S17. MS/MS spectrum of Palmitoleamide (**65, Table 1**).

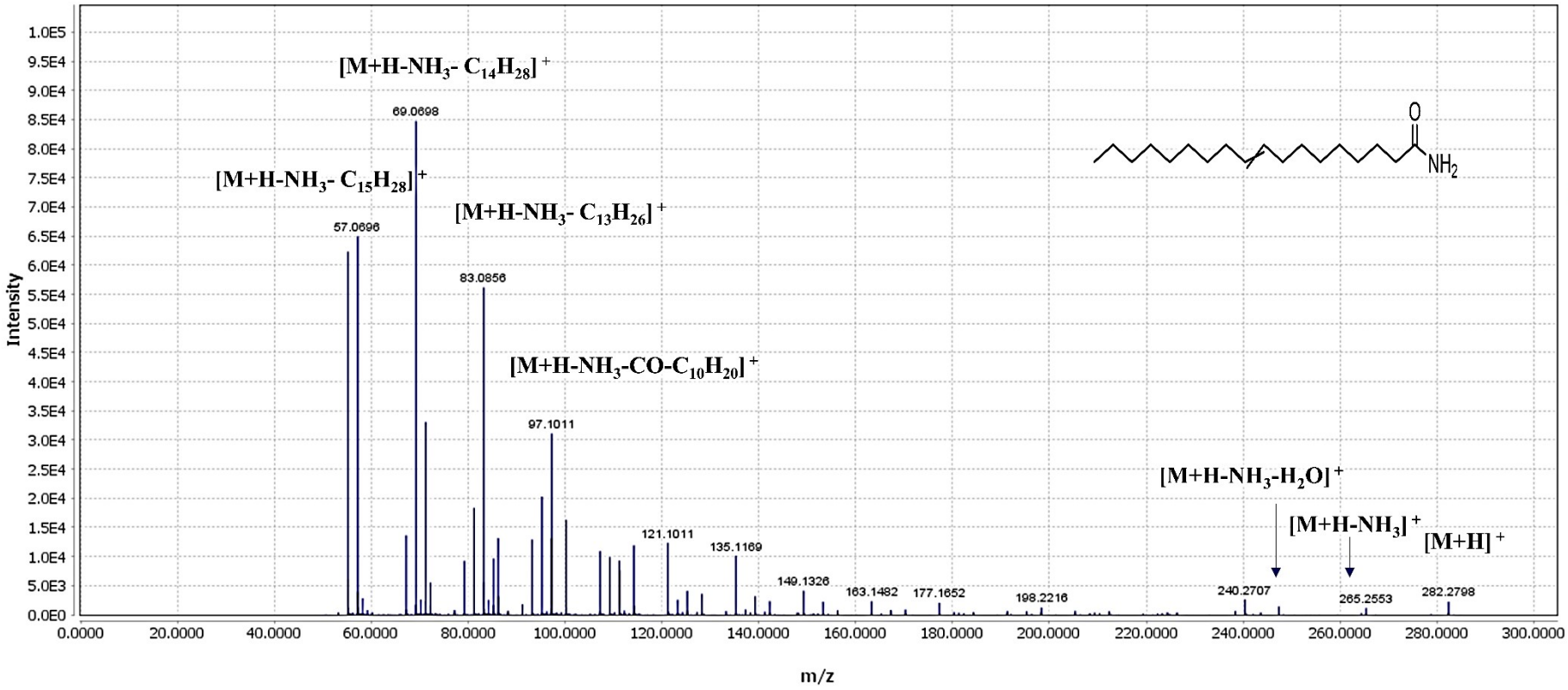

Fig. S18. MS/MS spectrum of octadecenamide (**78, Table 1**).

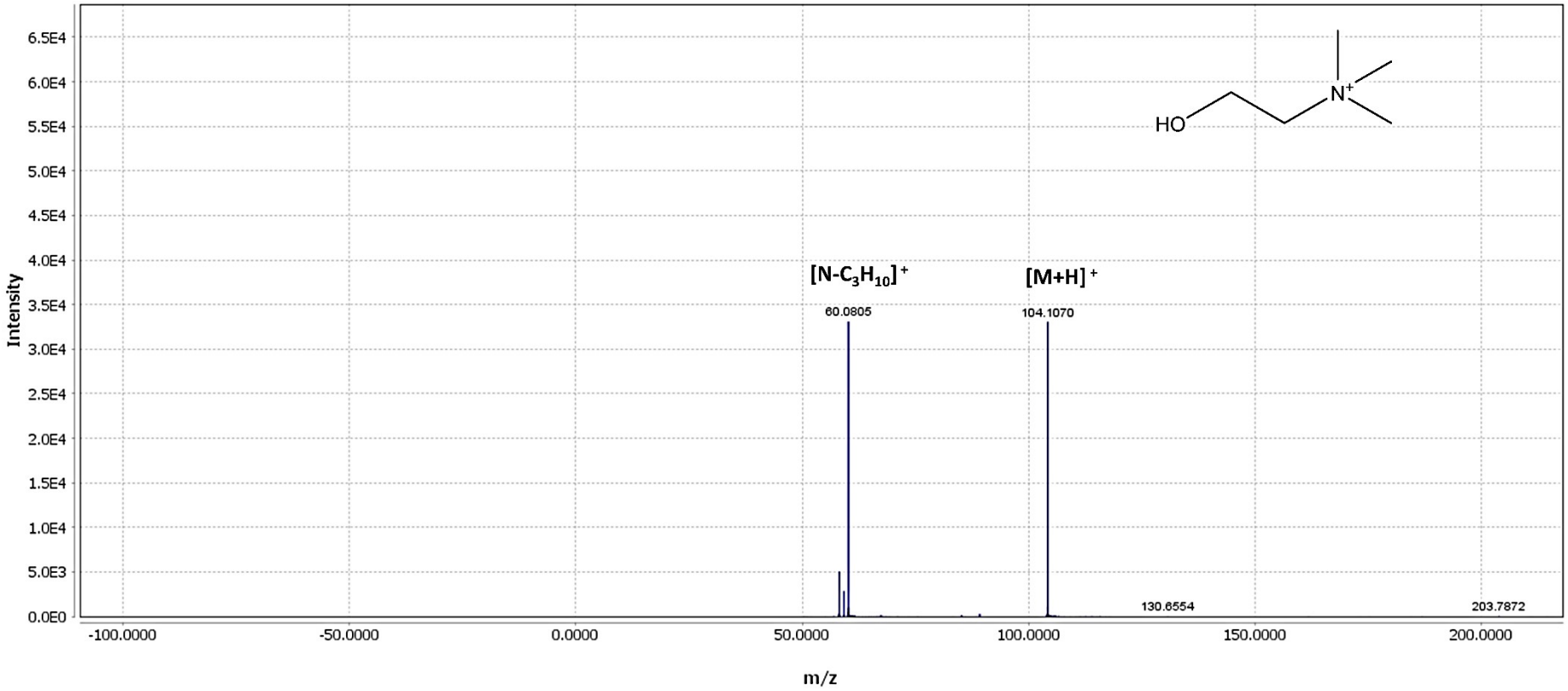

Fig. S19. MS/MS spectrum of choline (**6, Table 1**).

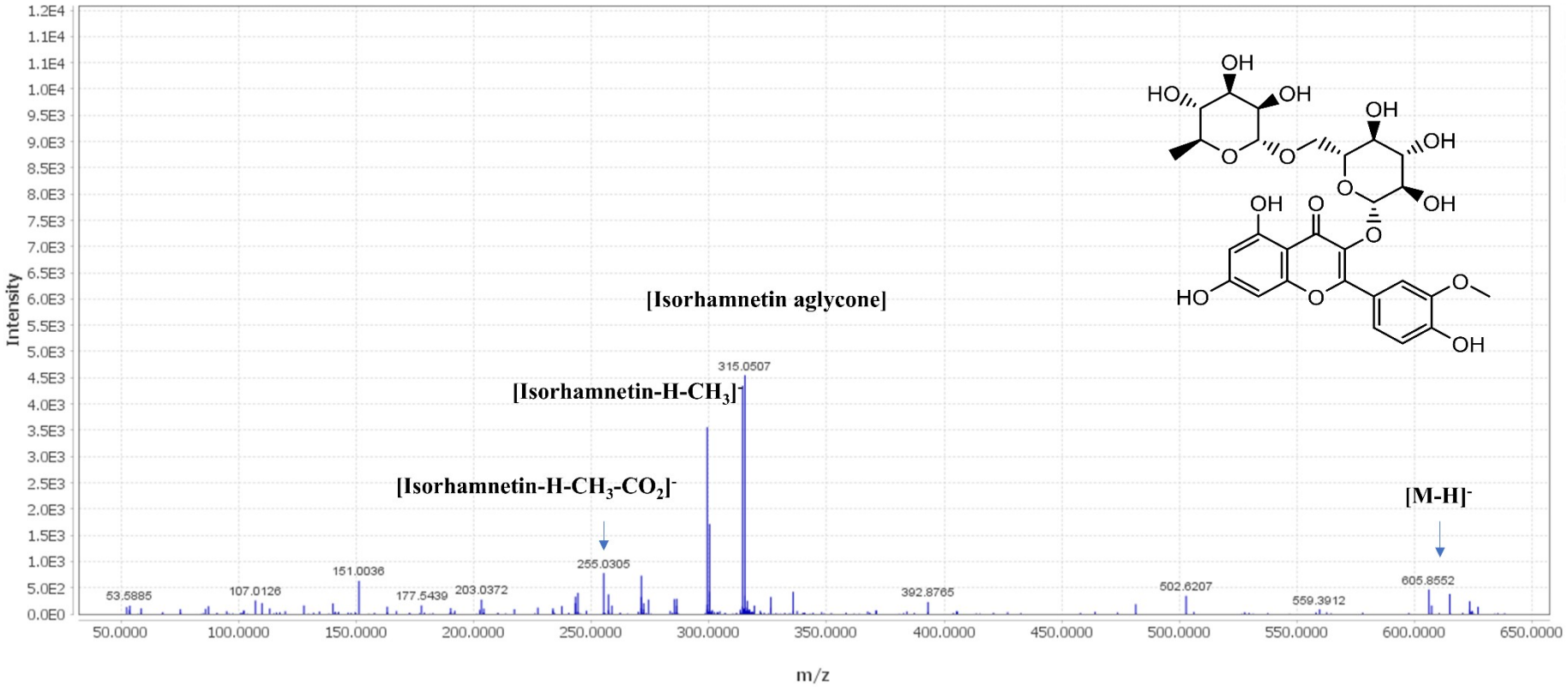

Fig. S20. MS/MS spectrum of isorhamnetin-3-*O*-rutinoside (**23, Table 1**).

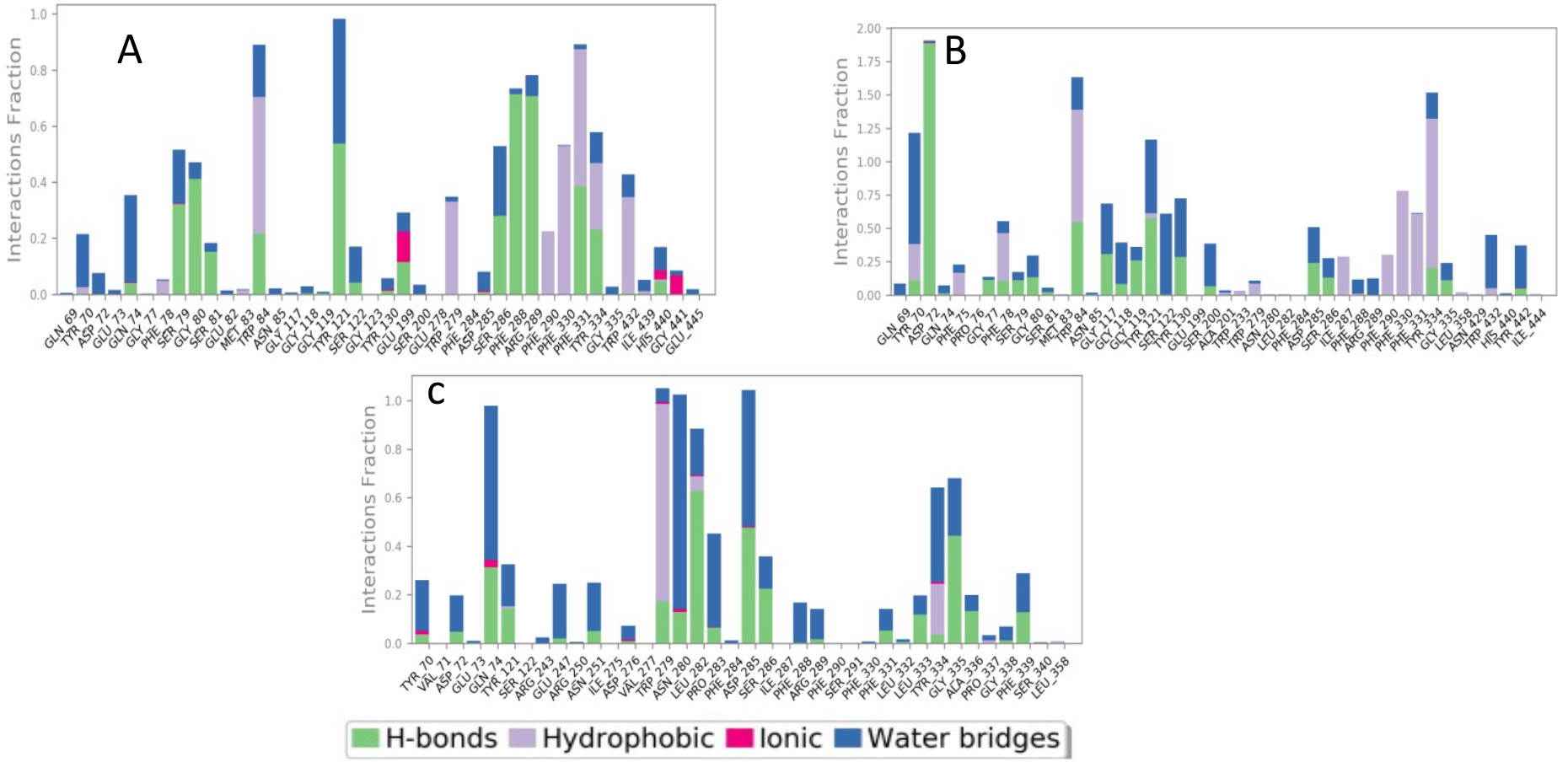

Figure S21. Histograms of for (**A**) Rosmarinic acid, (**B**) Sebestenoid, and (**C**) Sagerinic acid ligands within the binding site of acetylcholinesterase (1OCE) during the simulation time of 200 ns.

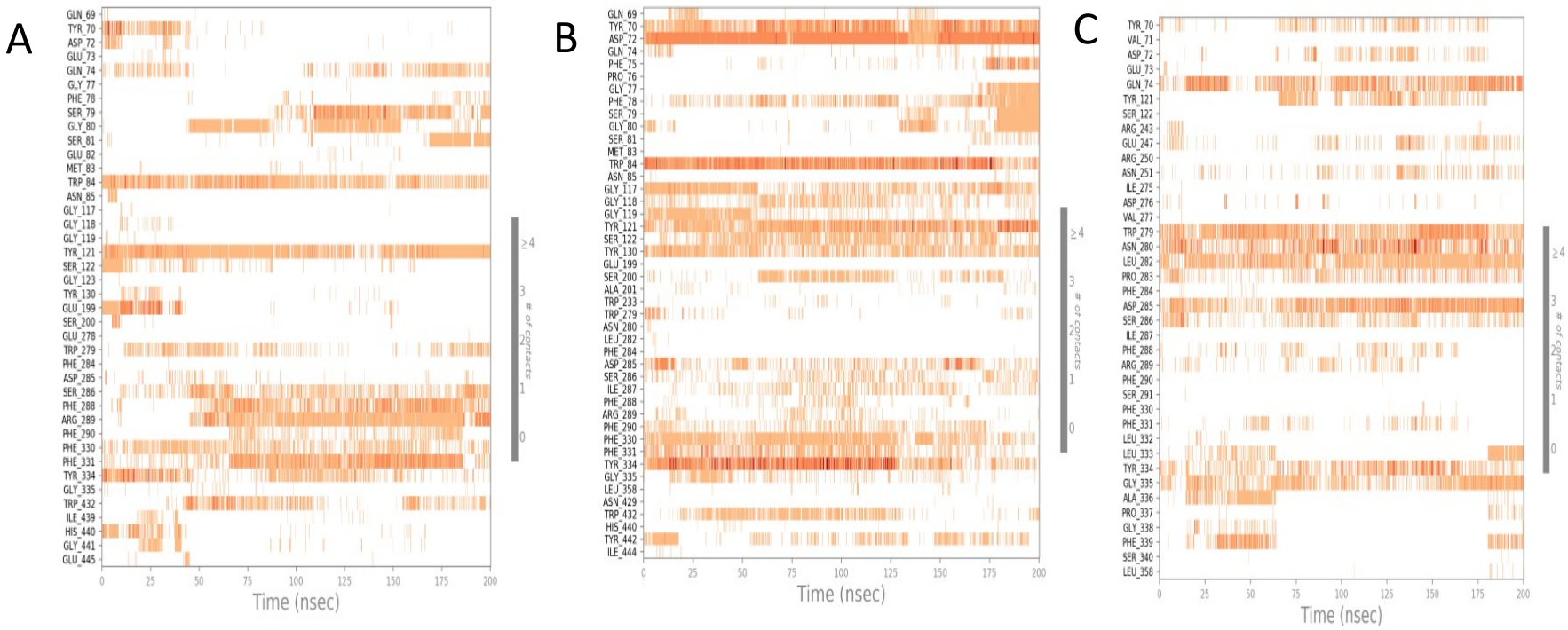

Figure S.22. Heat maps of (**A**) Rosmarinic acid, (**B**) Sebestenoid C, and (**C**) Sagerinic acid ligands within the binding site of acetylcholinesterase (1OCE) during the simulation time of 200 ns.

Reference list:

1 E. Harder, W. Damm, J. Maple, C. Wu, M. Reboul, J. Y. Xiang, L. Wang, D. Lupyan, M. K. Dahlgren, J. L. Knight, J. W. Kaus, D. S. Cerutti, G. Krilov, W. L. Jorgensen, R. Abel and R. A. Friesner, *J. Chem. Theory Comput.*, 2016, **12**, 281–296.

2 W. L. Jorgensen, J. Chandrasekhar, J. D. Madura, R. W. Impey and M. L. Klein, *J. Chem. Phys.*, 1983, **79**, 926–935.

3 E. Neria, S. Fischer and M. Karplus, *J. Chem. Phys.*, 1996, **105**, 1902–1921.

4 G. J. Martyna, M. L. Klein and M. Tuckerman, *J. Chem. Phys.*, 1992, **97**, 2635–2643.

5 G. J. Martyna, D. J. Tobias and M. L. Klein, *J. Chem. Phys.*, 1994, **101**, 4177–4189.